JACS
JOURNAL OF THE AMERICAN CHEMICAL SOCIETY
Article
pubs.acs.org/JACS

Columnar Self-Assemblies of Triarylamines as Scaffolds for Artificial Biomimetic Channels for Ion and for Water Transport

Susanne Schneider,[†,‡] Erol-Dan Licsandru,[§] Istvan Kocsis,[§] Arnaud Gilles,[§] Florina Dumitru,[§] Emilie Moulin,[‡] Junjun Tan,[‡] Jean-Marie Lehn,[†] Nicolas Giuseppone,*[,‡] and Mihail Barboiu*[,§]

[†]ISIS, Institut de Science et d'Ingénierie Supramoléculaires, 8 allée Gaspard Monge, 67000 Strasbourg, France

[‡]SAMS Research Group, University of Strasbourg, Institut Charles Sadron, CNRS, 23 rue du Loess, BP 84047, 67034 Strasbourg Cedex 2, France

[§]Adaptive Supramolecular Nanosystems Group, Institut Europèen des Membranes, ENSCM-UMII-CNRS UMR-5635, Place Eugène Bataillon, CC 047, F-34095 Montpellier, France

Supporting Information

ABSTRACT: Triarylamine molecules appended with crown-ethers or carboxylic moieties form self-assembled supramolecular channels within lipid bilayers. Fluorescence assays and voltage clamp studies reveal that the self-assemblies incorporating the crown ethers work as single channels for the selective transport of K^+ or Rb^+. The X-ray crystallographic structures confirm the mutual columnar self-assembly of triarylamines and crown-ethers. The dimensional fit of K^+ cations within the 18-crown-6 leads to a partial dehydration and to the formation of alternating K^+ cation-water wires within the channel. This original type of organization may be regarded as a biomimetic alternative of columnar K^+-water wires observed for the natural KcsA channel. Supramolecular columnar arrangement was also shown for the triarylamine-carboxylic acid conjugate. In this latter case, stopped-flow light scattering analysis reveals the transport of water across lipid bilayer membranes with a relative water permeability as high as 17 μm s^{-1}.

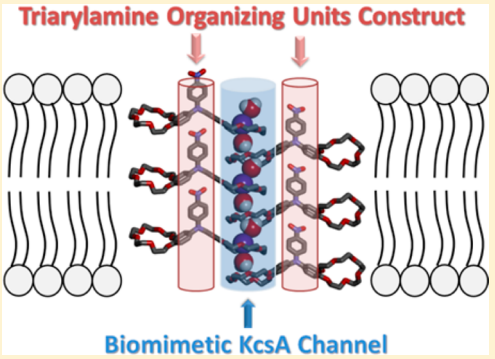

INTRODUCTION

Ion and water transport across lipid bilayers is one of the most important processes in living cells, which is supported by relatively simple biomolecular carriers and by more complex transmembrane protein channels.[1−3] It is well recognized that the study of artificial biomimetic transmembrane channels for ions and water is of crucial importance to understanding the translocation mechanisms of their natural counterparts. Furthermore, such artificial channels are of high applicative interest toward the design of novel drugs and sensors, as well as for the implementation of separation and delivery processes.[4−6] Originally, large single molecules spanning the lipid bilayers have been used to construct synthetic channels.[7−13] More recently, another very attractive strategy has been developed based on the self-assembly of several small building blocks toward the creation of supramolecular channels.[14,15] In this latter case, the dynamics (i.e., kinetic lability) of the self-assemblies can confer emerging properties to the channels, which can adapt their superstructures in response to external *stimuli* such as ionic gradients.[15] For instance, we have shown that gramicidin-A can be biomimicked using a simple synthetic bola-amphiphile triazole.[16] We have also constructed artificial aquaporins from ureido-imidazole compounds, formed via the self-assembly of Imidazole I-quartets, that can efficiently transport water and protons while excluding all other ions.[17] Finally, we have reported H-bonded self-assembled ion channels incorporating crown-ethers, in which the ion-translocation functions are dynamically associated with ionic recognition.[18−24] Pursuing our endeavors to design original supramolecular channels with efficient transport properties, we recently got interested in the possibility to make use of a directional structuring of the triarylamine platform. The molecular design of the present study is inspired by our recent findings showing that triarylamine molecules, when substituted with amide groups, are able to form supramolecular nanoarchitectures including rods,[25−27] fibers,[28−32] spheres,[33,34] either in solution, at interfaces,[35,36] or within a confined space.[37] However, the self-assembly of triarylamines has not yet been explored toward the generation of directional ion or water transporting channels within lipid bilayer membranes. We now report that compounds **1** and **2** (Figure 1) can self-assemble inside lipid bilayer membranes to form alkali cation or water channels, respectively.

RESULTS AND DISCUSSION

Alkali Metal Ion Transport. Among artificial cation transport systems, macrocyclic crown-ethers have already

Received: November 28, 2016
Published: February 16, 2017

DOI: 10.1021/jacs.6b12094
J. Am. Chem. Soc. 2017, 139, 3721−3727

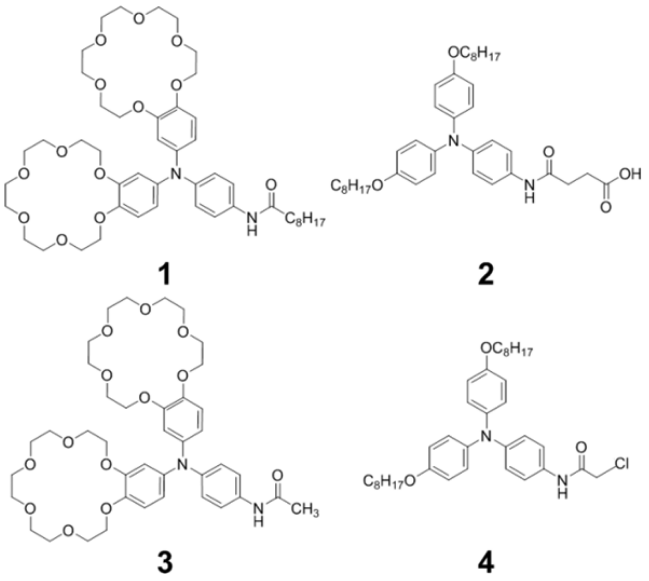

Figure 1. Chemical structures of triarylamines **1** and **2** used for alkali cation and water channels, respectively. Compounds **3** and **4** were used for control experiments to test the influence of the alkyl chain length and of the crown ether and carboxylic acid group presence on the transport efficiencies.

been studied as ion binder and translocator units, or as channel-forming blocks in bilayer membranes.[8,18−23,38,39] Compound **1** was synthesized in order to combine crown-ether binding properties with the directional self-assembly properties of triarylamines for the transport of alkali cations. The key step of the synthesis consists in a modified Ullman coupling reaction of *p*-nitroaniline with 4-bromobenzo-18-crown-6, and is followed by the introduction of hydrophobic nonanoylamide alkyl chains that are in principle favorable for the incorporation of compound **1** within the lipid bilayer membrane (see the Supporting Information section 1 for the synthetic procedures and Scheme S1).

First, ^{1}H NMR titration experiments in acetonitrile solutions at ambient temperature showed that compound **1** binds K^+ cations as well as Na^+ cations in a 1:2 binding stoichiometry, with the first binding constant two times higher in the case of K^+ ($K_{1K+} = 1.67 \times 10^6$) compared to Na^+ ($K_{1Na+} = 8.75 \times 10^5$). The second binding constants were shown to be 20 times weaker for potassium ($K_{1K+} = 8.47 \times 10^4$), and 10 times weaker for sodium ($K_{1Na+} = 7.68 \times 10^4$), relatively to the first ion binding (see the Supporting Information section 2, and Figures S1−S4).

Then, the transport of alkali metal ions through a lipid bilayer incorporating different concentrations of **1** was studied by a HPTS fluorescence assay on large unilamellar phosphatidylcholine vesicles.[40] In this method, the fluorescent probe HPTS (8-hydroxypyrene-1,3,6-trisulfonic acid, pK_a = 7.2), which in its protonated and deprotonated states exhibits two different absorption wavelengths (450 and 405 nm respectively), is used as a pH probe in order to indirectly measure the transport of alkali metal ions M^+ (Figure 2). After introduction of **1**, the addition of sodium hydroxide solution to the extravesicular medium creates a pH gradient of approximately one unit compared to the intravesicular medium. Mediated by **1**, this gradient can then be compensated by metal-ion/proton antiport or by metal-ion/hydroxide cotransport.[40,41] By monitoring the relative fluorescence intensity

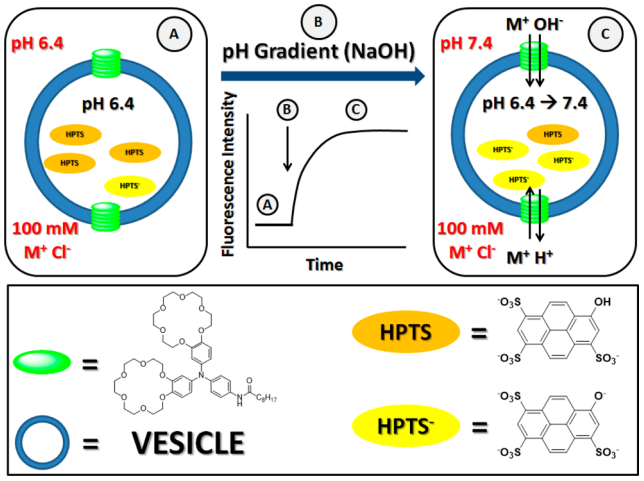

Figure 2. Schematic representation of the HPTS fluorescence assay for the study of metal ion transport through lipid bilayer membranes containing self-assembled compound **1**.

(I_{450}/I_{405}) of the HPTS probe, we measured an increase of the intravesicular pH which reflects the alkali metal ion transport across the membrane. Figure 3 shows the normalized fluorescence intensity ratios (Figure 2a and c) together with the fractional activities at 500 s (Figure 3b and d) for the selective transport of K^+ and Na^+ in the concentration range of 1 μM < [**1**] < 50 μM (final concentration in total amount of

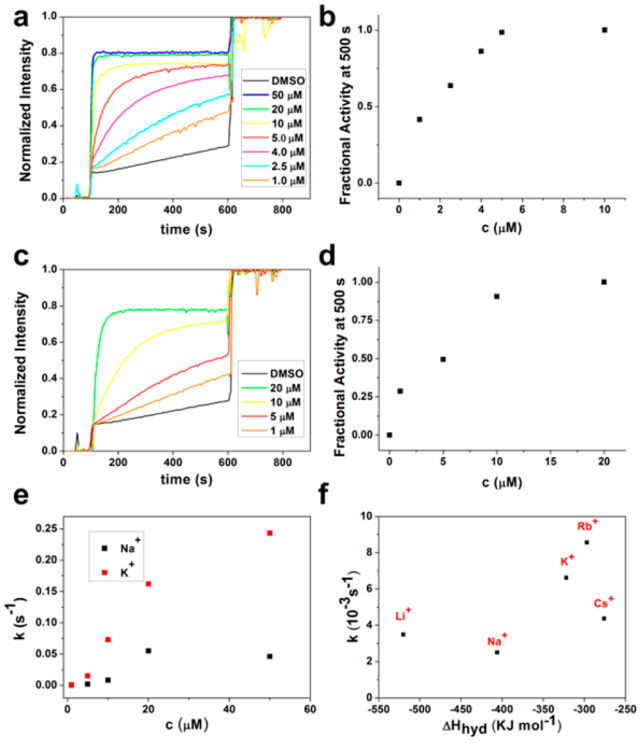

Figure 3. Changes in the fluorescence intensity ratio (I_{450}/I_{405}) as a function of time (a,c), and corresponding fractional activity at 500 s for different concentrations of **1** (b,d), for the transport of K^+ (a,b) and Na^+ (c,d) cations through egg yolk L-α-phosphatidylcholine (EYPC) bilayer vesicles. (e) Pseudo-first-order rate constants for the transport of K^+ and Na^+ cations at different concentrations of **1**. (f) Pseudo-first-order rate constants for the transport as a function of hydration free enthalpy of cation, for 5 μM of **1**.

DOI: 10.1021/jacs.6b12094
J. Am. Chem. Soc. 2017, 139, 3721−3727

vesicle suspension). Increasing the concentration of compound **1** from 20 to 50 μM hardly increases the transport activity at 500 s, indicating a saturation of the transport. On the basis of previous work that shows that some triarylamine monoamides can be self-assembled in solution on light irradiation,[25] we further tested whether the light promoted self-assembly of **1** (see Figures S5, S7, S8 and S9 in the Supporting Information) has a beneficial effect on the rate of ion transport.

We conducted two assays: adding the compound to the liposomes either before or after vesicle extrusion. In the first, premix, assay the self-assembled **1** was mixed with the lipids before the liposome formation. However, the extrusion of the vesicles was not possible due to the generation of a very thick slurry. In the postmix assay, in which the self-assembled channels were injected into preformed liposomes with the aid of dimethyl sulfoxide (DMSO) we obtained transport efficiencies very similar to that of the nonself-assembled channels (see Figure S13a–c in the Supporting Information). Irradiation of chloroform solutions of compound **1** leads to its self-assembly, however, after drying of the solutions in vacuo and dissolution of the assembled structures in DMSO, the light induced self-assembled structures decompose into its monomeric building blocks as can be seen from its NMR spectra (see Supporting Information Figure S11). We believe that the entrapment of compound **1** inside the lipid bilayer membrane forces it into its active, channel functional structure, due to a combination of $\pi-\pi$ stacking, hydrogen bonding, van-der-Waals as well as hydrophobic interactions within the lipid bilayer,[42] thus making the light-induced self-assembly unnecessary in order to achieve effective cation transport.

The preference toward the transport of K^+ versus Na^+ is shown by the higher pseudo-first-order rate constants obtained for the whole concentration domain (Figure 3e). For the alkali cations series, the transport activity increases in the order $Li^+ \sim Na^+ < K^+ \sim Rb^+$, very close to the Eisenman sequence I and corresponding to the energetic penalty for ion dehydration (Figure 3f and Figure S14 in the Supporting Information).[43] It is emphasizing that the sandwich Rb^+ (18-crown-6)$_2$ complex does not inhibit or lower the conductance of a crown-stack channel. Cs^+ cation showed a much lower conductance compared to K^+ and Rb^+, in agreement with the lower ion-channel binding behaviors of Cs^+ which is much bigger than and less adapted to the 18-crown-6 macrocyclic cavity to form sandwich complexes.

Initially, we presumed that the presence of long nonanoylamide chains grafted to the triarylamine core of compound **1** would be beneficial to its hydrophobic incorporation inside the lipid bilayer. However, compound **3** (Figure 1), which instead of the long nonanoylamide chain is modified with a less hydrophobic acetylamide chain, shows the same efficiency of transport toward K^+ (Figure S13d). Thus, the insertion of **1** or **3** mainly relates on the columnar self-assembly of the triarylamine cores. To determine whether the presence of a self-assembling triarylamine core itself is sufficient for transport, we tested the activity of compound **4**[25] (Figure 1), which does not contain crown ether groups. The inactivity of **4** for the transport of K^+ (Figure S13d) shows that the triarylamine core is not by itself responsible for the ion transport, and that the presence of a crown ether group is mandatory.

Planar bilayer conductance measurements[44] were then performed using KCl as an electrolyte (Figure 4, Figure S15 in the Supporting Information). The data revealed the top

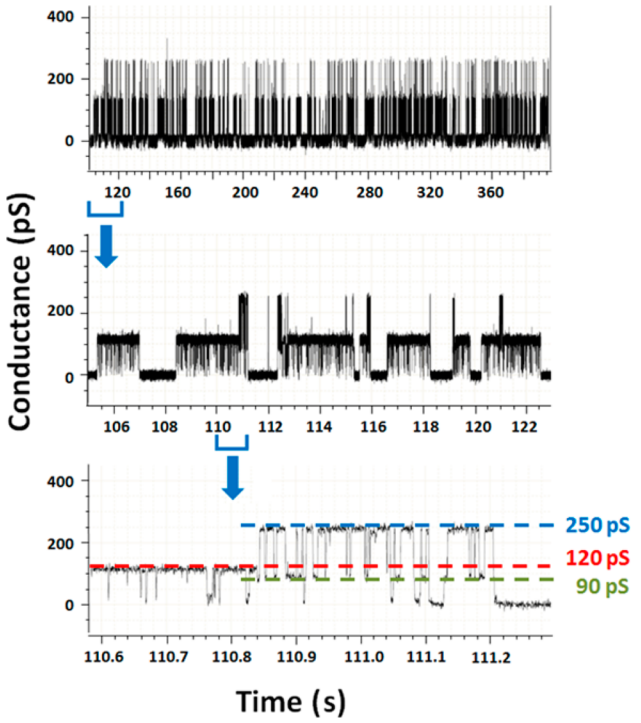

Figure 4. Single channel behavior of **1** measured by planar bilayer conductance for the following conditions: 1 M KCl *cis* and *trans* side, 100 mV applied potential. Different magnification of the same trace: 5 min (top), 18 s (middle) and 720 ms (bottom).

square activity of **1**, with quite long opening times of the channel. However, some flickering behavior was also observed, probably due to inherent dynamics of the supramolecular construction. From this recording that lasted for more than 2 h from the onset of activity, it has been possible to observe two main opened states, each of them containing two subsets that participate approximately for half to each of the main conductance state (Figure 5). At a first glance, one can suggest that the two main conductance levels would correspond to two independent channel openings, but a third channel opening was never observed. Moreover, the open probability of the second main level of conductance lies far below the open probability of the first one (4.5% vs 44.5%). A last observation is that this

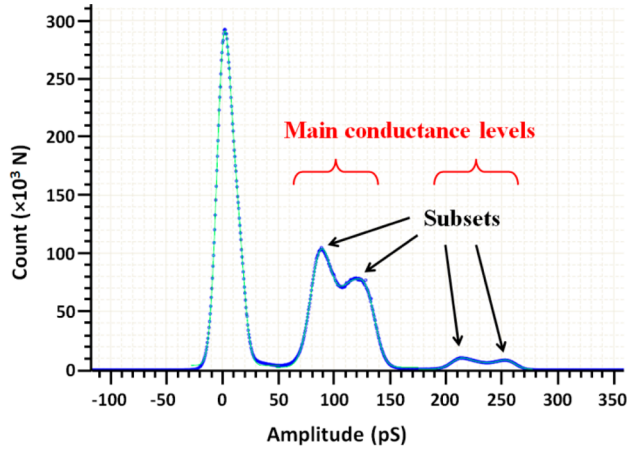

Figure 5. Histogram of a 120 min voltage clamp recording (blue) and Gaussian fit (green) of the potassium channel openings of **1**.

DOI: 10.1021/jacs.6b12094
J. Am. Chem. Soc. 2017, 139, 3721–3727

second main level was opened only at the same time as one of the subsets of the first level (Figure 4 bottom). This is consistent with the fact that the second opening occurs on the same self-assembly, and that the second crown ether present on compound **1** is either creating a second channel or contributes to the formation of a bigger channel when all the crown ethers are "synchronized". Thus, the main level conductance is approximately 90 pS, which corresponds to an opened diameter of 4.8 Å (corrected Hille estimation).[45] Subsets have a conductance level of 28 pS, which would correspond to an open pore of 2.6 Å diameter, being too low to permit the passage of the potassium ion (1.7 Å radius). This subset therefore corresponds to a second open form of the main first conductance level, with a value of 120 pS, i.e., 5.6 Å in pore diameter. Thus, the different conductance levels probably arise from two conformational states of the same active superstructure.

We were further interested in obtaining evidence on the structural self-assembly of the crown-ether-triarylamines into channel-type superstructures. Although attempts at crystallizing compound **1** failed, we were able to crystallize its nitro precursor (**ii** in the Supporting Information) by evaporation of an acetonitrile/water solution of **ii** in the presence of KTf (Figure 6). The asymmetric unit cell contains two molecules of **ii** with a K^+ cation bound to one of the four 18-crown-6-ethers. The cell contains also four water molecules out of which two are coordinated to K^+, as well as 2 molecules of acetonitrile and two half molecules of triflate anions. In the solid state the K^+ is equatorially coordinated by the 18-crown-6 ring with a nearly planar D_{3d} conformation (average $d_{K\cdots O}$ = 2.80 Å). Both apical positions of K^+ are occupied by the bridging water molecules ($d_{O\cdots K}$ of 2.80 Å), which are simultaneously H-bonded to the neighboring crown-ether-triarylamines. The view along the crystallographic *b* axis, reveals the formation of the $K^+\cdot H_2O$ filled channels, with K^+ cations and H_2O molecules alternatively lined to every second crown ether moiety along the macrocyclic columnar channel (Figure 6a). The view along the crystallographic *a* axis reveals the coaxial structure of each triarylamine column with a nitrogen−nitrogen distance of d_{N-N} = 9.3 Å and the slightly displaced overlapping of the crown ethers which are disposed at a $d_{crown-crown}$ = 4.6 Å interval within the columnar self-assembly (Figure 6b).

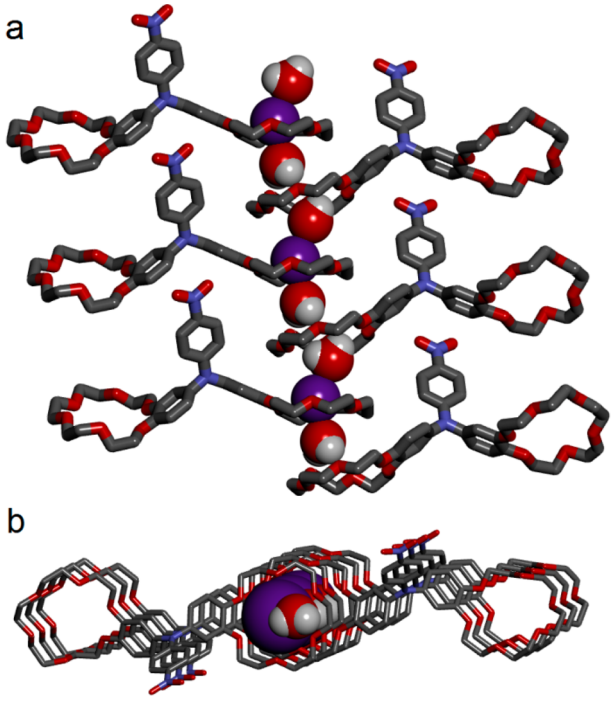

Figure 6. Crystal structure in stick representation of the crown-ether-triarylamine compound **ii** complexed with KTf; (a) the K^+ channel that is formed by alternation of $K^+\cdot H_2O$ wires along the crown-ether stacks of intertwined crown-ether-triarylamine channel-arrays along the *b*-axis and (b) the parallel alignment of crown-ether-triarylamine molecules along the *a*-axis. K^+ and H_2O molecules are represented in CPK. All protons of compound **ii** have been omitted for clarity.

We were also able to obtain single crystals suitable for X-ray analysis of compound **ii** in the absence of K^+ by slow evaporation of a methanol/water solution (Figure 7). The asymmetric unit cell contains one molecule of **ii** together with 14 molecules of water (from which one has been squeezed out). The structure contains multiple H-bonding interactions between the water and the oxygen atoms of the 18-crown-6-ether groups. The view down the *a*-axis (Figure 7a) shows that the triarylamine cores are coaxial, with a nitrogen−nitrogen distance of d_{N-N} = 8.84 Å and a parallel alignment of the crown ethers. In contrast to the previous **ii**·K^+ superstructure, the two crown ethers on the same triarylamine core point in opposite directions (Figure 7b). In addition, it can be seen that crown ethers from neighboring molecules do not overlap along the *b*-axis and create collateral water containing triarylamine channels (Figure 7c).

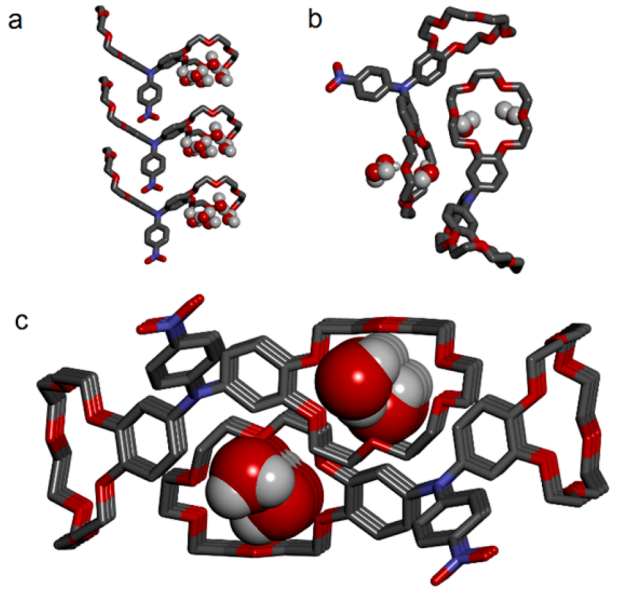

Figure 7. Crystal structure of the crown-ether-triarylamine compound **ii** in the absence of K^+; stick presentation of (a) the uniaxial alignment of the triarylamine cores; (b) the two crown-ethers present on the same molecule pointing in opposite directions as compared to a *cis* configuration for the complexed compound; and (c) the view along the crystallographic *b*-axis revealing the tight packing of adjacent crown ethers of neighboring molecules resulting in the formation of hydrated channels. H_2O molecules are represented in CPK. All protons of compound **ii** have been omitted for clarity.

Although the three-dimensional networks formed by the two complexes present key differences, both crystal structures indicate that the triarylamines can self-assemble into uniaxial directional columnar arrays. In its uncomplexed state, the

DOI: 10.1021/jacs.6b12094
J. Am. Chem. Soc. 2017, 139, 3721−3727

triarylamine cores are already preorganized in a channel like conformation, while the presence of K^+ cations bound to the crown-ether moieties generates a much more ordered network. In addition, several crystals obtained from cocrystallization of compound **ii** in the presence of different amounts of NaTf always revealed the structure of the uncomplexed compound **ii**, which is in agreement with the weaker binding affinity of 18-crown-6 ethers toward Na^+ cations.

Although very attractive, these structures cannot provide direct molecular-level insights into the functional dynamics of these channels in the lipid membrane environment. However, the steric disposition of the translocated solutes is strongly reminiscent of that observed for the active gate filter of the natural K^+ KcsA channel: the K^+ cations and H_2O molecules are alternatively positioned to overcome the electrostatic destabilization along the channel and to provide K^+-H_2O cotranslocation.[46,47] A very similar artificial structure has been published by Lehn et al. in 1982: a polymolecular stack of crown-ethers are stabilizing K^+-H_2O wires, "as in a frozen picture of potassium ion propagation through the stack".[48] This solid state channel-type structure represents a fantastic similarity with K^+-H_2O wires identified by MacKinnon et al. within the natural KcsA channel in 1998.[46] Later similar examples relate to H_3O^+/H_2O[49] or Na^+/H_2O[50] translocation through dibenzo-18-crown-ether channels through single-crystals. We believe that the structure reported in this paper is one of the first artificial examples displaying such a structural similarity to the natural KcsA channel and presenting ion-channel conductance states in bilayer membranes.

In the literature, it is known that the cation translocation within a bilayer membrane environment occurs via a macrocyclic site-to-site jumping mechanism, with the optimal distance between two individual crown ether sites being 6 Å and the maximal distance being 11 Å.[8] We also further determined a distance of 4.8 Å between two urea-H-bonded 15-crown-5-ether sites to allow the formation of a $K^+\cdot[15\text{-crown-5-ether}]_2$ sandwich complex which is favored through multivalent binding sites despite the energetic loss upon recovering the hydration sphere of the cation.[23] This situation seems to be different for the sterically hindered 18-crown-6-ether moieties that are grafted onto the triarylamine backbones at an interval of $d_{crown-crown}$ = 4.6 Å. In this case, a sandwich complex is not the favored morphology. Instead, the $K^+\cdot H_2O$ [18-crown-6-ether] adopts a rather constrained geometry in which the binding of the apical water molecules compensates for the energetic loss caused by the dehydration of the potassium during the equatorial binding with the 18-crown-6-ether moieties. Moreover, the Na^+ cations are too small to fit with a proper coordination to the 18-crown-6-ether groups, thus preventing the formation of a constrained $Na^+\cdot H_2O$ [18-crown-6-ether] geometry. This has been confirmed by the fact that we were unable to obtain crystals of **ii**·Na^+.

Water Transport. To test whether triarylamines can be used as a general building block toward the construction of self-assembled channels for transport within lipid bilayers, we synthesized compound **2** (Figure 1) from primary amine **iii**[25] and succinic anhydride (Scheme S2). Compound **2** contains a free carboxylic acid which we expected to transport water via hydrogen bonding interactions. All the compounds studied in this paper have been tested for their water transport activity, but there was no observed activity besides compound **2**. Natural K^+ empty KscA channels are often far better at transporting water than cations, allowing water transport 20 time faster than one-dimensional bulk diffusion of water.[51] Certainly, the X-ray crystal structure of the crown analogs in K^+/water (Figure 6) and water-filled (Figure 7) channels, suggests that it should be a good water transporter. Despite tempting structures, there was no observed water transport activity for the macrocyclic compounds **1** and **3**.

A common technique to analyze the water flux through water channels is based on stopped-flow light scattering: the bilayer vesicles are subject to a change in osmolarity, causing a change of vesicle size, which will then result in a change of the light scattering intensity.[52] Thus, vesicles prepared from a phosphatidylcholine/phosphatidylserine/cholesterol mixture (molar ratio 4/1/5) were rapidly subjected to an outwardly oriented osmotic gradient (i.e., 200 mM sucrose inside the vesicles and 400 mM sucrose outside). Under these conditions, a reduction in vesicle volume due to water efflux leads to an increase in the light scattering signal at 90° which is further normalized (Figure 8a).

According to the Rayleigh–Gans theory, the system can be fitted by an exponential function and the osmotic water permeability (P_f) can be calculated using eq 1:

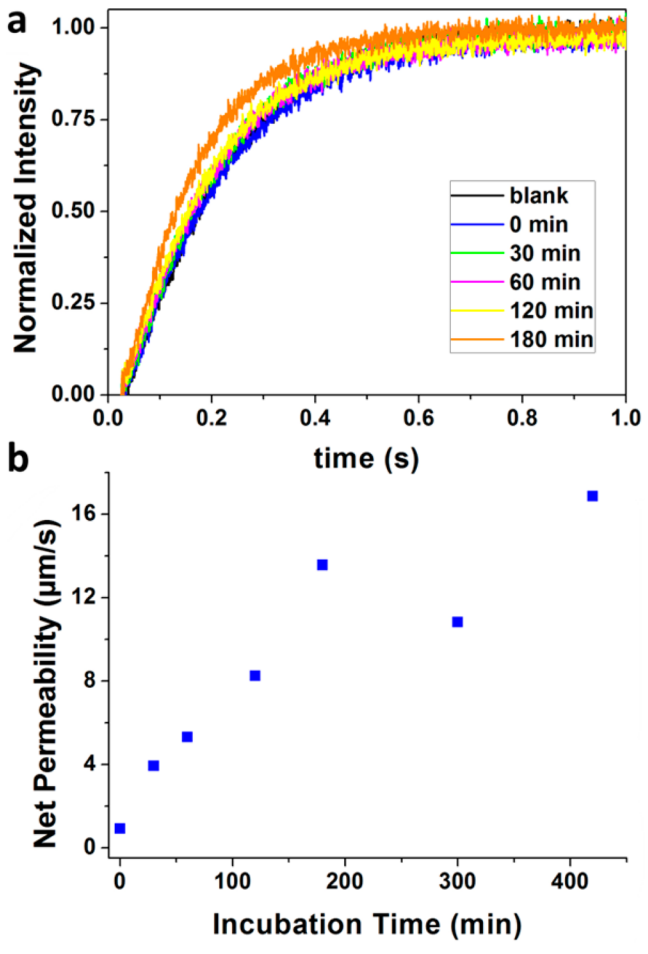

Figure 8. (a) Normalized stopped-flow light scattering traces after different incubation times of phosphatidylcholine/phosphatidyl serine/cholesterol (molar ratio 4/1/5) vesicles with an optimal 100 μM total concentration of 2 and lipid to compound **2** molar ratio LCR = 4 and the application of an osmotic gradient; (b) average net water permeabilities of the vesicles after varying times of incubation with **2**, obtained from exponential fitting of the light scattering results.

DOI: 10.1021/jacs.6b12094
J. Am. Chem. Soc. 2017, 139, 3721–3727

$$P_f = \frac{k}{\frac{S}{V_0} \times V_w \times \Delta_{osm}} \quad (1)$$

there k is the exponential coefficient of the change in the light scattering, S and V_0 are the initial surface area and volume of the vesicles, respectively, V_w is the molar volume of water, and Δ_{osm} is the osmolarity difference.[51]

Compound **2** is not soluble in water as proven by NMR experiments. We thus presume a total distribution of **2** in the bilayer membrane with an optimal total concentration of 100 μM. Lower or higher concentrations show low activity or precipitation of **2**, respectively. Unexpectedly, it was found that the water permeability depends on the time of incubation of the vesicles with **2**, prior to the creation of an osmotic gradient. Until 180 min of incubation, net permeabilities increase almost linearly, reaching values about 13 μm s^{-1}, which corresponds to a 25% increase of the permeability compared to the background transport of vesicles in the absence of **2** and a 15 times larger permeability in the case of using **2** but without incubation. If incubated for longer times, the permeability can be as high as 17 μm s^{-1}. This indicates that the evolving channel formation might be related to a relatively slow self-assembly process for compound **2** within the bilayer membrane. The fact that permeabilities change slightly between 180 and 420 min might be attributed to the intrinsic stabilized nature of the channel systems. As in the case of metal ion transport by compound **1**, the light-induced self-assembled structure of compound **2** (Figures S6 and S10 in the Supporting Information) decompose into its monomeric building blocks when in DMSO (Figure S12 in the Supporting Information), but inside the lipid bilayer membrane is forced it into its active, functional channel structure as a result of noncovalent interactions. In addition, no water transport was detected for triarylamine **4**, thus indicating that the carboxylic groups are the effectors for the water transport.

In order to get an idea of the supramolecular assembly of compound **2** we were again interested in obtaining single crystals suitable for X-ray analysis. In order to do so, we synthesized the methyl-analogue of **2** (compound **v** in the Supporting Information) assuming that the high anisotropy caused by the long alkyl chains hinders the molecule from crystallizing. After more than a month of slow layer diffusion of a cyclohexane/tetrahydrofuran solution of **v** in a NMR tube we obtained crystals suitable for X-ray analysis. Surprisingly, the structure revealed that **v** had undergone an intramolecular cyclization, resulting in the formation of a succinimide (Figure 9).

The view along the crystallographic c-axis reveals a columnar stacking of a repeating motif of two triarylamine units with a "snow-flake" arrangement, as has already been reported for other triarylamine crystals and which is in agreement with the predicted triarylamine arrangement (in absence of bulky groups such as crown ethers).[27,31] The uniaxial alignment of compound **v** displays the appended succinimide groups at d_{N-N} = 4.62 Å, the stacking distance of two molecules. Although the structure obtained of **v** is not compound **2**, we believe that the triarylamine with the free carboxylic acid and long alkyl chains creates a two-dimensional structure that can bridge the lipid bilayer membrane to form water channels. However, we cannot exactly assume the same packing behaviors in order to estimate the composition and the number of channels in the membrane in order to determine the exact

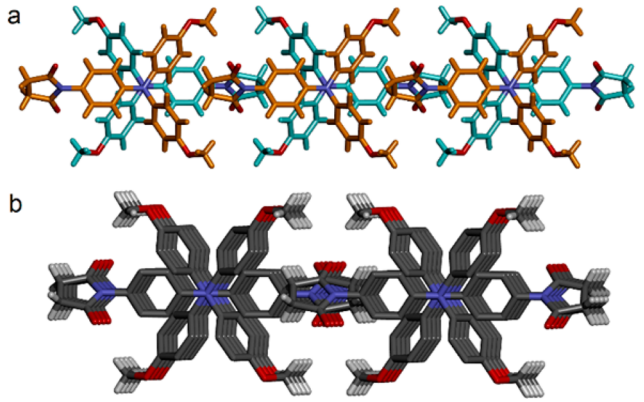

Figure 9. Crystal structure of the methoxy analogue of compound **v** (see the Supporting Information) after intramolecular succinimide formation, stick presentation (a) showing an uniaxial alignment of the triarylamines with a nitrogen−nitrogen distance (d_{N-N} = 4.62 Å) and (b) displaying the stacking motif of two molecules along the columnar axis in the "snowflake" arrangement. Protons of the triarylamine core have been omitted for clarity.

permeability/channel as previously reported.[42] UPLC analysis of compound **2** after 24 h in DMSO displays no significant formation of the succinimide, thus we can relate the measured water permeability completely to the free acid.

In summary, we have demonstrated that artificial membrane-spanning channels can be constructed based on supramolecular triarylamine scaffolds. Transport experiments show that these superstructures can display cation- and water-conductance behaviors. The single-crystal structures reveal in both cases that the channel arrangements are afforded by the columnar packing of the triarylamine molecules. In addition, X-ray crystallography shows that the dimensional fit of K^+ cations induce a H_2O binding ability by stacked crown-ether sites, which leads to $K^+ \cdot H_2O$ filled channels. This has important consequences for the selective $K^+ \cdot H_2O$ cotranslocation which compensates the electrostatic destabilization along the channel. It reveals a very interesting biomimetism with the K^+ KcsA channel. Overall, the present work extends the broad potential of triarylamines as supramolecular construction units in general, and within the confined space of lipid bilayers in particular. The facile and modular synthesis of the triarylamine platform affords in principle a large variety of possibilities to finely tune the function and activity of this new family of supramolecular transmembrane channels.

■ ASSOCIATED CONTENT

Supporting Information

The Supporting Information is available free of charge on the ACS Publications website at DOI: 10.1021/jacs.6b12094.

Synthetic protocols and characterization of triarylamine compounds, ^{1}H NMR titration results, ^{1}H NMR and UV−vis spectra for self-assembly studies, supplementary HPTS and stopped-flow data, X-ray crystal structure data and general procedures (PDF)

X-ray crystal file for **ii** (CIF)

X-ray crystal file for **ii**·KTf (CIF)

X-ray crystal file for **v** (CIF)

DOI: 10.1021/jacs.6b12094
J. Am. Chem. Soc. 2017, 139, 3721−3727

AUTHOR INFORMATION

Corresponding Authors

*giuseppone@unistra.fr
*mihail-dumitru.barboiu@univ-montp2.fr

ORCID

Jean-Marie Lehn: 0000-0001-8981-4593
Nicolas Giuseppone: 0000-0003-4093-3000
Mihail Barboiu: 0000-0003-0042-9483

Notes

The authors declare no competing financial interest.

ACKNOWLEDGMENTS

This work was supported by funds from ITN DYNANO, PITN-GA-2011-289033 (http://www.dynano.eu) and from ANR DYNAFUN, ANR-15-CE29-0009-02. We would like to thank the X-ray crystallographic unit of the University of Strasbourg for the analysis of the crystal structures. We would like to thank the website http://new.supramolecular.org for providing the software Bindfit.

REFERENCES

(1) Saier, M. H. *J. Membr. Biol.* **2000**, *175*, 165−180.
(2) King, L. S.; Kozono, D.; Agre, P. *Nat. Rev. Mol. Cell Biol.* **2004**, *5*, 687−698.
(3) Cukierman, S. *Biophys. J.* **2000**, *78*, 1825−1834.
(4) Sisson, A. L.; Shah, M. R.; Bhosale, S.; Matile, S. *Chem. Soc. Rev.* **2006**, *35*, 1269.
(5) Lehn, J.-M. In *Physical Chemistry of Transmembrane Ion Motions*; Spach, G., Ed.; Elsevier: Amsterdam, 1983; pp 181−207.
(6) MacKinnon, R. *Angew. Chem., Int. Ed.* **2004**, *43*, 4265−4277.
(7) Gokel, G. W.; Murillo, O. *Acc. Chem. Res.* **1996**, *29*, 425−432.
(8) Otis, F.; Racine-Berthiaume, C.; Voyer, N. *J. Am. Chem. Soc.* **2011**, *133*, 6481−6483.
(9) Shen, Y.-X.; Si, W.; Erbakan, M.; Decker, K.; De Zorzi, R.; Saboe, P. O.; Kang, Y. J.; Majd, S.; Butler, P. J.; Walz, T.; Aksimentiev, A.; Hou, J.; Kumar, M. *Proc. Natl. Acad. Sci. U. S. A.* **2015**, *112*, 9810−9815.
(10) Jullien, L.; Lehn, J.-M. *Tetrahedron Lett.* **1988**, *29*, 3803−3806.
(11) Weiss, L. A.; Sakai, N.; Ghebremariam, B.; Ni, C.; Matile, S. *J. Am. Chem. Soc.* **1997**, *119*, 12142−12149.
(12) Montenegro, J.; Ghadiri, M. R.; Granja, J. R. *Acc. Chem. Res.* **2013**, *46*, 2955−2965.
(13) Kaucher, M. S.; Harrell, W. A.; Davis, J. T. *J. Am. Chem. Soc.* **2006**, *128*, 38−39.
(14) Barboiu, M. *Angew. Chem., Int. Ed.* **2012**, *51*, 11674−11676.
(15) Lehn, J.-M. *Angew. Chem., Int. Ed. Engl.* **1988**, *27*, 89−112.
(16) Barboiu, M.; Le Duc, Y.; Gilles, A.; Cazade, P.-A.; Michau, M.; Marie Legrand, Y.; van der Lee, A.; Coasne, B.; Parvizi, P.; Post, J.; Fyles, T. *Nat. Commun.* **2014**, *5*, 4142.
(17) Le Duc, Y.; Michau, M.; Gilles, A.; Gence, V.; Legrand, Y.-M.; van der Lee, A.; Tingry, S.; Barboiu, M. *Angew. Chem., Int. Ed.* **2011**, *50*, 11366−11372.
(18) Gilles, A.; Barboiu, M. *J. Am. Chem. Soc.* **2016**, *138*, 426−432.
(19) Sun, Z.; Barboiu, M.; Legrand, Y.-M.; Petit, E.; Rotaru, A. *Angew. Chem., Int. Ed.* **2015**, *54*, 14473−14477.
(20) Sun, Z.; Gilles, A.; Kocsis, I.; Legrand, Y. M.; Petit, E.; Barboiu, M. *Chem. - Eur. J.* **2016**, *22*, 2158−2164.
(21) Barboiu, M.; Cerneaux, S.; Van Der Lee, A.; Vaughan, G. *J. Am. Chem. Soc.* **2004**, *126*, 3545−3550.
(22) Cazacu, A.; Tong, C.; van der Lee, A.; Fyles, T. M.; Barboiu, M. *J. Am. Chem. Soc.* **2006**, *128*, 9541−9548.
(23) Barboiu, M.; Vaughan, G.; van der Lee, A. *Org. Lett.* **2003**, *5*, 3073−3076.
(24) Cazacu, A.; Legrand, Y.-M.; Pasc, A.; Nasr, G.; Van der Lee, A.; Mahon, E.; Barboiu, M. *Proc. Natl. Acad. Sci. U. S. A.* **2009**, *106*, 8117−8122.
(25) Moulin, E.; Niess, F.; Maaloum, M.; Buhler, E.; Nyrkova, I.; Giuseppone, N. *Angew. Chem., Int. Ed.* **2010**, *49*, 6974−6978.
(26) Jouault, N.; Moulin, E.; Giuseppone, N.; Buhler, E. *Phys. Rev. Lett.* **2015**, *115*, 1−5.
(27) Nyrkova, I.; Moulin, E.; Joseph, J.; Armao, I.; Maaloum, M.; Heinrich, B.; Rawiso, M.; Niess, F.; Cid, J.-J.; Jouault, N.; Buhler, E.; Semenov, A. N.; Giuseppone, N. *ACS Nano* **2014**, *8*, 10111−10124.
(28) Armao, J. J.; Maaloum, M.; Ellis, T.; Fuks, G.; Rawiso, M.; Moulin, E.; Giuseppone, N. *J. Am. Chem. Soc.* **2014**, *136*, 11382−11388.
(29) Wolf, A.; Moulin, E.; Cid, J.-J.; Goujon, A.; Du, G.; Busseron, E.; Fuks, G.; Giuseppone, N. *Chem. Commun.* **2015**, *51*, 4212−4215.
(30) Domoto, Y.; Busseron, E.; Maaloum, M.; Moulin, E.; Giuseppone, N. *Chem. - Eur. J.* **2015**, *21*, 1938−1948.
(31) Armao, J. J.; Rabu, P.; Moulin, E.; Giuseppone, N. *Nano Lett.* **2016**, *16*, 2800−2805.
(32) Faramarzi, V.; Niess, F.; Moulin, E.; Maaloum, M.; Dayen, J.-F.; Beaufrand, J.-B.; Zanettini, S.; Doudin, B.; Giuseppone, N. *Nat. Chem.* **2012**, *4*, 485−490.
(33) Moulin, E.; Niess, F.; Fuks, G.; Jouault, N.; Buhler, E.; Giuseppone, N. *Nanoscale* **2012**, *4*, 6748−6751.
(34) Busseron, E.; Cid, J.-J.; Wolf, A.; Du, G.; Moulin, E.; Fuks, G.; Maaloum, M.; Polavarapu, P.; Ruff, A.; Saur, A.-K.; Ludwigs, S.; Giuseppone, N. *ACS Nano* **2015**, *9*, 2760−2772.
(35) Armao, J. J.; Domoto, Y.; Umehara, T.; Maaloum, M.; Contal, C.; Fuks, G.; Moulin, E.; Decher, G.; Javahiraly, N.; Giuseppone, N. *ACS Nano* **2016**, *10*, 2082−2090.
(36) Armao, J. J., IV; Nyrkova, I.; Fuks, G.; Osypenko, A.; Maaloum, M.; Moulin, E.; Arenal, R.; Semenov, A.; Giuseppone, N. *J. Am. Chem. Soc.* **2017**, *139*, 2345−2350.
(37) Licsandru, E.-D.; Schneider, S.; Tingry, S.; Ellis, T.; Moulin, E.; Maaloum, M.; Lehn, J.-M.; Barboiu, M.; Giuseppone, N. *Nanoscale* **2016**, *8*, 5605−5611.
(38) Gokel, G. W. *Chem. Commun.* **2000**, 1−9.
(39) Fyles, T. M. *Chem. Soc. Rev.* **2007**, *36*, 335−347.
(40) Sidorov, V.; Kotch, F. W.; Abdrakhmanova, G.; Mizani, R.; Fettinger, J. C.; Davis, J. T. *J. Am. Chem. Soc.* **2002**, *124*, 2267−2278.
(41) Benke, B. P.; Madhavan, N. *Chem. Commun.* **2013**, *49*, 7340.
(42) Licsandru, E.; Kocsis, I.; Shen, Y.; Murail, S.; Legrand, Y.-M.; van der Lee, A.; Tsai, D.; Baaden, M.; Kumar, M.; Barboiu, M. *J. Am. Chem. Soc.* **2016**, *138*, 5403−5409.
(43) Eisenmann, G.; Horn, R. J. *J. Membr. Biol.* **1983**, *76*, 197−225.
(44) Matile, S.; Sakai, N.; Hennig, A. In *Supramolecular Chemistry*; John Wiley & Sons, Ltd., 2012.
(45) Smart, O. S.; Breed, J.; Smith, G. R.; Sansom, M. S. P. *Biophys. J.* **1997**, *72*, 1109−1126.
(46) Doyle, D. A.; Morais Cabral, J.; Pfuetzner, R. A.; Kuo, A.; Gulbis, J. M.; Cohen, S. L.; Chait, B. T.; MacKinnon, R. *Science* **1998**, *280*, 69−77.
(47) Köpfer, D. A.; Song, C.; Gruene, T.; Sheldrick, G. M.; Zachariae, U.; de Groot, B. L. *Science* **2014**, *346*, 352−355.
(48) Behr, J. P.; Lehn, J. M.; Dock, A. C.; Borras, D. *Nature* **1982**, *295*, 526−527.
(49) Fromm, K. M.; Gueneau, E. D.; Geosmann, H.; Bochet, C.G. Z. *Z. Anorg. Allg. Chem.* **2003**, *629*, 597−600.
(50) Fromm, K. M.; Berbougnant, R. D. *Solid State Sci.* **2007**, *9*, 580−587.
(51) Saparov, S. M.; Pohl, P. *Proc. Natl. Acad. Sci. U. S. A.* **2004**, *101*, 4805−4809.
(52) Borgnia, M. J.; Kozono, D.; Calamita, G.; Maloney, P. C.; Agre, P. *J. Mol. Biol.* **1999**, *291*, 1169−1179.

DOI: 10.1021/jacs.6b12094
J. Am. Chem. Soc. 2017, 139, 3721−3727